For the purpose of showcasing the image deposition process to the BioImage Archive for a workshop in 'Trends in Microscopy 2025', this document contains a shortened version of the following paper:

Dynamic multi-omics and mechanistic modeling approach uncovers novel mechanisms of kidney fibrosis progression

Nadine Tuechler, Mira Lea Burtscher, Martin Garrido-Rodriguez, Muzamil Majid Khan, Denes Türei, Christian Tischer, Sarah Kaspar, Jennifer Jasmin Schwarz, Frank Stein, Mandy Rettel, Rafael Kramann, Mikhail M Savitski, Julio Saez-Rodriguez, Rainer Pepperkok

bioRxiv 2024.10.15.618507; doi: https://doi.org/10.1101/2024.10.15.618507

Dynamic multi-omics and mechanistic modeling approach uncovers novel mechanisms of kidney fibrosis progression

Nadine Tuechler [1,2,3], Mira Lea Burtscher [1,3], [...] Rainer Pepperkok [1,2]

1 European Molecular Biology Laboratory (EMBL), Heidelberg, Germany
2 Molecular Medicine Partnership Unit (MMPU), European Molecular Biology Laboratory and Heidelberg University, Heidelberg, Germany
3 Heidelberg University, Faculty of Medicine, and Heidelberg University Hospital, Institute for Computational Biomedicine (ICB), Heidelberg, Germany

Nadine Tüchler
E-mail: nadine.tuechler@embl.de
Role: first author
ORCID: 0000-0002-8125-3098
Affiliations

- European Molecular Biology Laboratory
- Molecular Medicine Partnership Unit (MMPU), European Molecular Biology Laboratory and Heidelberg University, Heidelberg, Germany
- Heidelberg University

Mira Burtscher
E-mail: mira.burtscher@embl.de
Role: first author
ORCID: 0000-0003-2628-0795
Affiliations

- European Molecular Biology Laboratory
- Heidelberg University

Rainer Pepperkok
E-mail: pepperko@embl.de

Role: corresponding author
ORCID: 0000-0002-9762-3583
Affiliations

- European Molecular Biology Laboratory
- Molecular Medicine Partnership Unit (MMPU), European Molecular Biology Laboratory and Heidelberg University, Heidelberg, Germany

Abstract
Kidney fibrosis, characterized by excessive extracellular matrix deposition, is a progressive disease that, despite affecting 10% of the population, lacks specific treatments and suitable biomarkers. This study presents a comprehensive, time-resolved multi-omics analysis of kidney fibrosis using an in vitro model system based on human kidney PDGFRβ+ mesenchymal cells aimed at unraveling disease mechanisms. Using transcriptomics, proteomics, phosphoproteomics, and secretomics we quantified over 14,000 biomolecules across seven time points following TGF-β stimulation. This revealed distinct temporal patterns in the expression and activity of known and potential kidney fibrosis markers and modulators. Data integration resulted in time-resolved multi-omic network models which allowed us to propose mechanisms related to fibrosis progression through early transcriptional reprogramming. Using siRNA knockdowns and phenotypic assays, we validated predictions and regulatory mechanisms underlying kidney fibrosis. In particular, we show that several early-activated transcription factors, including FLI1 and E2F1, act as negative regulators of collagen deposition and propose underlying molecular mechanisms. This work advances our understanding of the pathogenesis of kidney fibrosis and provides a resource to be further leveraged by the community.

Keywords: kidney fibrosis, extracellular matrix, multi-omics, time points, network modeling

Introduction
[...]

Results

2.1 Phenotypic and molecular features defining fibrosis in PDGFRβ+ mesenchymal cells over time
In this study, we present a comprehensive investigation of kidney fibrosis using an in vitro model system that enables detailed phenotypic and molecular disease characterization and has previously been used in the context of kidney fibrosis research (Kuppe et al. 2021). The use of human PDGFRβ+ mesenchymal cells in this tissue culture setup enables the induction of fibrotic differentiation with accelerated collagen deposition and ECM remodeling aer stimulation with TGF-β (Chen et al. 2009; Coentro et al. 2021; Khan et al. 2023; Rønnow et al. 2020). This system not only enables the time-resolved characterization of the phenotypic and molecular features of fibrotic processes, but also facilitates subsequent perturbation and validation (Figure 1A).

Within 96 hours of TGF-β stimulation, we observed a robust fibrosis-like phenotype as shown by COL1 secretion (Figure 1B, Figure S1A, B), morphological changes (actin stress fiber formation, Figure S1C) and SMAD2/3 phosphorylation (Figure S2). Quantification of the extracellular COL1 fluorescence intensity revealed a significant increase of COL1 deposition upon TGF-β stimulation aer 24 hours compared to the corresponding control at 24 hours, while we also observed increased collagen levels in the control conditions likely due to the macromolecular crowding agent and ascorbic acid used to accelerate collagen deposition (Figure 1C). This highlights the accelerated time scale in which a fibrosis-like phenotype can be achieved with this setup.

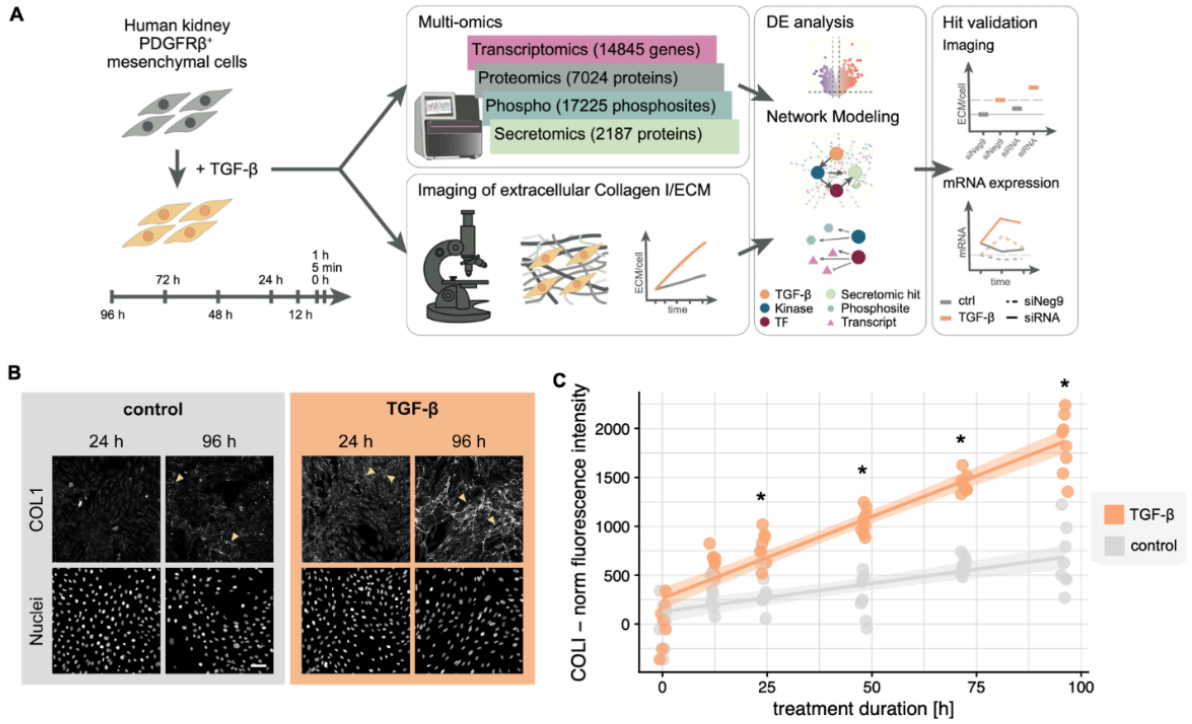

Figure 1: Phenotypic and molecular features defining fibrosis in PDGFRβ+ mesenchymal cells.

(A) Overview of experimental and bioinformatic strategy. Human kidney PDGFRβ+ mesenchymal cells were treated with 10 ng/ml TGF-β for 5 min (0.08 h), 1, 12, 24, 48, 72, 96 h. Investigation of extracellular matrix changes over time and multi-omics data integration via mechanistic modeling. Factors of interest were further validated.

(B) Immunofluorescence staining of extracellular COL1 and nuclei are shown at 96 h in control (macromolecular crowding + ascorbic acid) and TGF-β (TGF-β + macromolecular crowding + ascorbic acid) treated condition. Arrows highlight fibrillar collagen. Scale bar = 100 µm.

(C) Extracellular COL1 fluorescence intensity over the specified time points and treatment conditions. Quantification of COL1 fluorescence staining was performed following background correction, correction for cell autofluorescence, and normalization to nuclei number. Single replicates are depicted by the dots (n = 36 images are averaged per replicate). Data was square root transformed for statistical analysis using a linear mixed model (* corresponds to p-value < 0.05).

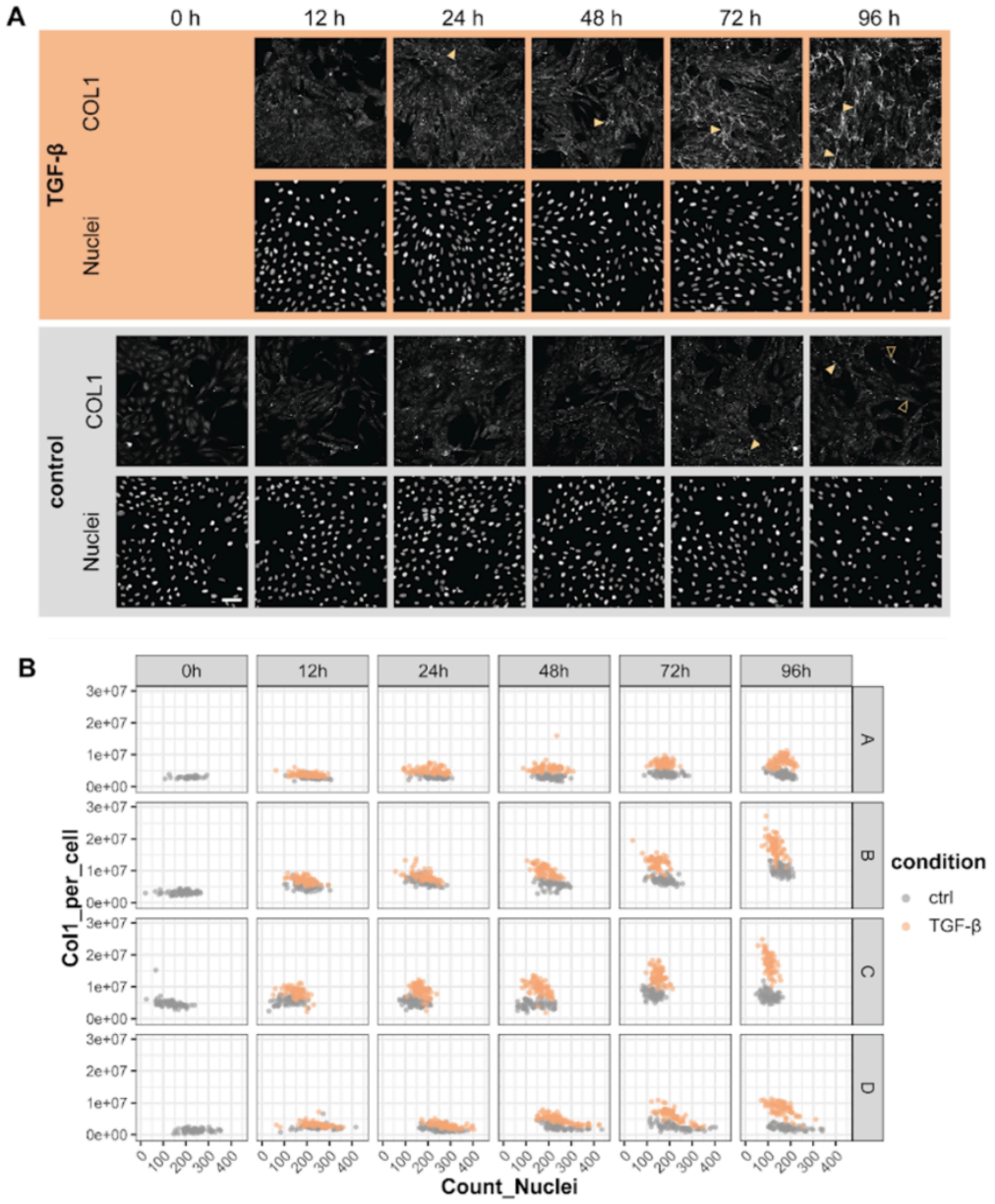

Supplementary Figure 1
(A) Widefield microscopy images showing COL1 (top rows) and nuclear (Hoechst, bottom rows) staining in control and TGF-β-treated conditions at 0, 12, 24, 48, 72, and 96 hours. (B) Quantification of COL1 expression per cell over time. Cells were cultured in four biological replicates (A-D) ± TGF-β for 0-96 h. Data points represent individual images, color coded for control (grey) and TGF-β (orange) conditions. Y-axis shows normalized COL1 intensity per cell, x-axis shows nuclei count per image. Images with less than 20 nuclei were excluded from the analysis.

[...]

2.4 Experimental validation confirms the implication of selected TFs in regulating ECM deposition

To further validate the role of these transcription factors in the development of fibrotic diseases, we exploited the perturbability of the used in vitro model system. We investigated their role in ECM remodeling and collagen deposition using siRNA knockdowns and subsequent imaging of the deposited ECM. By monitoring ECM production, we took advantage of a direct phenotypic readout of the knockdown performed, while RT-qPCR experiments allowed us to track the effects of TF knockdowns on the mRNA expression of their targets at the molecular level (Figure 4A, Table S9).
Analysis of the fluorescence intensity of the deposited ECM aer knockdown of the early activated TFs revealed a general trend towards increased deposition compared to a siNeg9 control (Figure 4B, Figure S6A). This effect is considerably pronounced upon TGF-β stimulation, indicating the importance of these TFs as potential negative regulators of collagen secretion given fibrotic signaling (Figure 4B, Figure S6A right panel). All six TF knockdowns had a significant impact on ECM deposition (unpaired two-sided t-test, p-value < 0.05), but for NR4A1 the effect magnitude was quite small, while the HNF4G knockdown was the only example that showed an opposite effect.

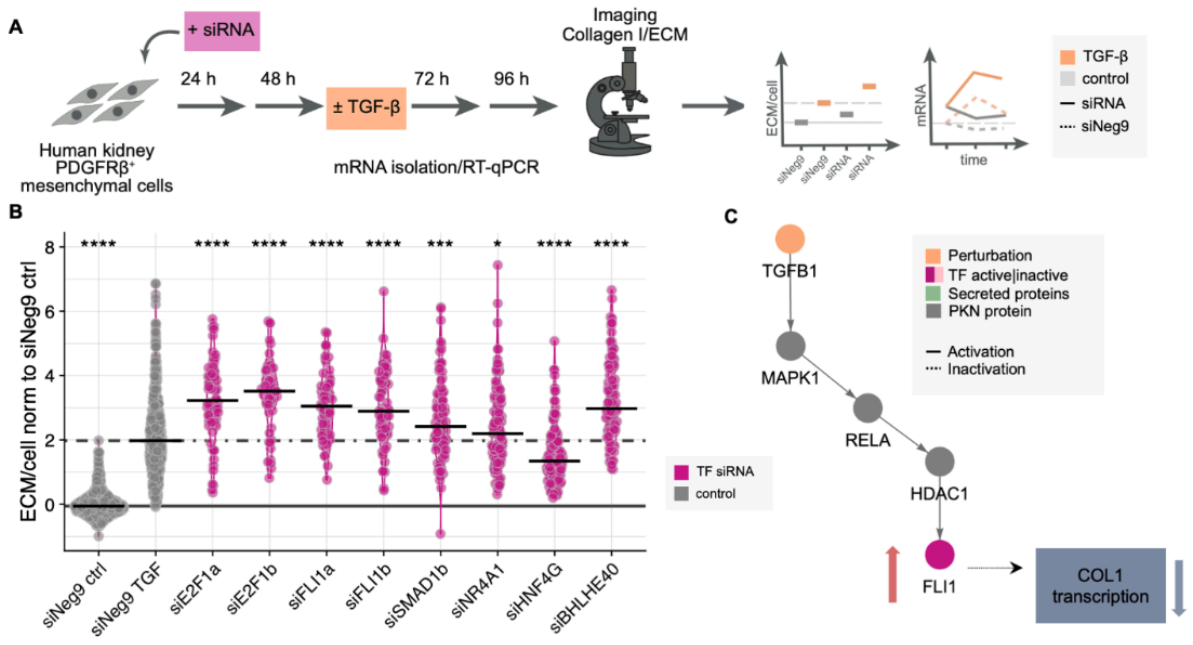

Figure 4: Validation of predicted fibrosis modulators and related molecular mechanisms.
(A) Schematic representation of the experimental workflow for validation experiments.
(B) Fluorescence intensity of ECM for selected TF knockdowns (purple, 96h knockdown followed by 48h TGF-β treatment) and the siNeg9 TGF-β treated/unstimulated controls (gray). Intensities of each knockdown were compared to the siNeg9 TGF-β treated condition (siNEg9 TGF) using a unpaired two-sided t-test (* corresponds to p-value < 0.05, ** corresponds to p-value < 0.01, *** corresponds to p-value < 0.001). Black bars represent the median fluorescence intensity per distribution.

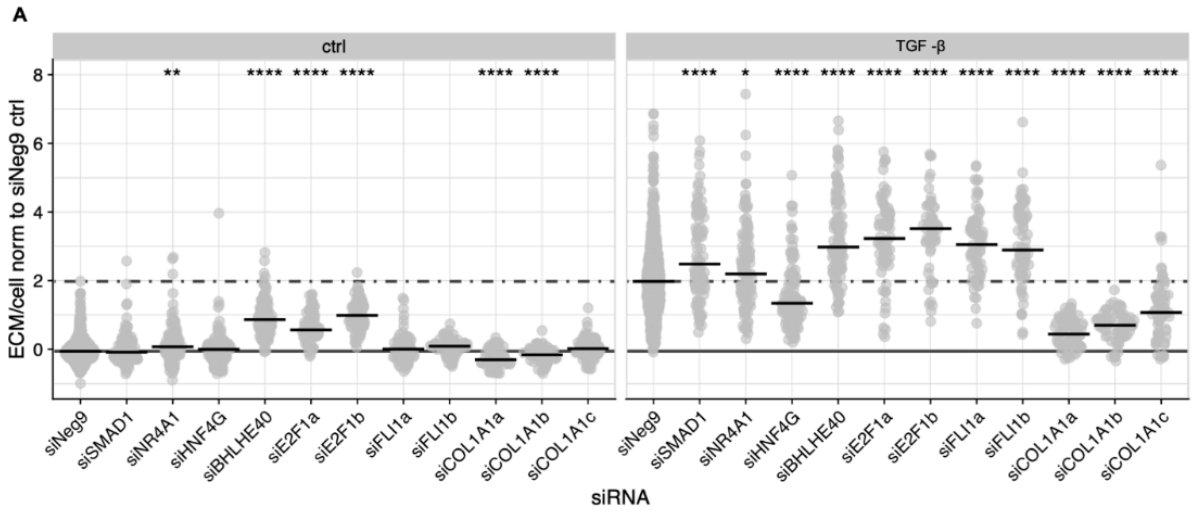

Supplementary Figure 6
(A) Fluorescence intensity of ECM for both untreated (ctrl) and TGF-β stimulated conditions for all performed knockdowns (96h knockdown followed by 48h +/- TGF-β treatment). Intensities of each knockdown were compared to the siNeg9 control condition (+/- TGF-β treatment) using a t-test (*corresponds to p-value < 0.05, ** corresponds to p-value < 0.01, *** corresponds to p-value < 0.001). For panels B-D and F, color indicates TGF-β stimulation (orange) vs control (gray). Line type distinguishes between siNeg9 control (solid) and target gene knockdown (dashed).

[...]

4. Materials and Methods

4.1 Cell Biology

Cell Lines and Reagents

Human kidney PDGFRβ+ mesenchymal cells were received from the Kramann lab (for further information please check (Kuppe et al. 2021)) and cultured in low glucose DMEM growth medium (Gibco 31885) supplemented with 5% FBS (Gibco A5256701). Cells were maintained at 37°C in a humidified incubator with 5% CO2 and passaged approximately three times a week. Mycoplasma testing was routinely conducted, yielding negative results.

Experimental Setup

For multi-omics and time point experiments, the medium in all conditions was changed 24 hours post-plating. The longest time point treatment (e.g. 96 hours) was initiated the day aer seeding. Control samples were maintained in low glucose DMEM without phenol red (Gibco 11880), supplemented with 1% L-Glutamine (Sigma Life Science G7513), Ficoll 70 and 400 (Sigma Aldrich F2878 and F4375), and 500 µM L-ascorbic acid 2-phosphate (Cayman Chemical Company 16457). TGF-β treated samples received the same medium with an additional 10 ng/ml of recombinant human TGF-β1 (R&D systems 240-B-010). Until the treatment started and for the 0 h treatments, the cells were kept in DMEM without phenol

red, FBS, Ficoll or ascorbic acid. Media changes were performed daily, with specific treatments applied as described to ensure all samples were ready for downstream processing at the same time.

siRNA Transfections

All siRNAs used are described in Table S7 and were acquired from Ambion/Thermo Fisher. Cells were plated one day before siRNA transfections, targeting 40-50% confluency on the day of treatment. The ScreenFect®siRNA protocol was employed. For a single 24-well plate reaction, 1 µl of ScreenFect®siRNA reagent (ScreenFect S-4001) was mixed with 39 µl of Dilution Buffer (ScreenFect S-2001). Separately, 5 pmol siRNA was diluted with 39 µl of Dilution Buffer. The mixtures were combined, incubated for 20 minutes at room temperature, and then 420 µl of fresh DMEM (without FBS) was added. The transfection mixture replaced the cell medium, which was changed to DMEM + 5% FBS aer 5-6 hours. For knockdown and TGF-β treatment experiments, cells were cultured for 48 hours post-siRNA transfection in DMEM + 5% FBS before starting TGF-β treatments, with media changes every 24 hours. Cells were fixed/harvested at specified time points.

Immunofluorescence Assays

Cells were seeded on glass-bottom 24-well plates (Cellvis P24-1.5H-N) and treated as described above. Aer aspirating the medium, cells were washed with PBS and fixed with 4% PFA (Thermo Fisher Scientific 50-980-491) containing 1:1000 Hoechst 33342 (Thermo Fisher Scientific H21492) for 10-15 minutes at room temperature. Following three PBS washes, cells were used for immunofluorescence staining.

Extracellular Immunofluorescence Staining

For extracellular matrix (ECM) visualization, cells were incubated with anti-COL1 antibody (Rockland 600-401-103-0.5, 1:500 in PBS) for 1-1.5 hours at room temperature, washed, and then incubated with fluorescently labeled secondary anti-rabbit IgG AlexaFluor 488 (Molecular Probes A11008, 1:400 in PBS) in PBS for 30-45 minutes. Washed cells were kept in PBS and imaged. Due to issues with new batches of the anti-COL1 antibody, GFP-labeled CNA35 dye (EMBL protein expression facility, 1:250 in PBS) was used for validation experiments (siRNA knockdowns of TFs). Aer fixation and washing, cells were incubated with CNA35 for 1-1.5 hours, washed, and imaged. In cases of increased autofluorescence from siRNA transfection, cells were stained with an anti-GFP (Origene TP401) followed by Alexa 647-conjugated secondary anti-rabbit (Invitrogen A21245).

[...]

4.2 Microscopy

Wide-field Microscopy

High-throughput imaging was conducted using the Molecular Devices IXM automated widefield screening microscope. A total of 36 fields of view were captured per well using a CFI P-Apo 20x Lambda/0.75 objective. Nuclear signals were acquired in the Hoechst

channel (Ex: 377/50, Em: 477/60), with ECM signals in the GFP channel (Ex: 472/30, Em: 520/35) or other channels depending on the secondary antibody used (such as Cy5 with Ex:28/40-25 Em: 692/40-25).

[...]

4.5 Data analysis

If not stated otherwise statistical analysis was performed using the R programming language (version 4.4.1) in the RStudio environment (version 2024.04.2+764).

Image Analysis of Wide-Field Microscopy Images

Image inspection and analysis, including nuclei segmentation and fluorescence quantification, were performed using Fiji ImageJ (Schindelin et al. 2012) and CellProfiler (Stirling et al. 2021). Details of the CellProfiler pipeline and parameters are provided in the Github repository (CellProfiler Pipeline). Key steps included image loading, channel assignment, nuclei segmentation, and fluorescence measurement. Data was exported to CSV files for downstream analysis.
CellProfiler output was imported into R (R Foundation for Statistical Computing 2021) for further analysis. Treatments were assigned based on well and position information extracted from the filenames. Fluorescence intensity values were rescaled and background subtracted. Autofluorescence and non-fibrillar ECM staining corrections were applied. Intensity values were then normalized to the number of nuclei in each image, calculating a per-nucleus intensity value. Images with low nuclei counts were excluded from the analysis.

COL1 deposition analysis

A linear mixed model with random intercept was applied to analyze COL1 deposition over time, accounting for treatment (TGF-β or control), time (0, 12, 24, 48, 72, and 96 h), and their interaction as fixed effects, with plate (biological replicate) set as random effect. The model formula in R notation is:

$$sqrt\_mean\_intensity \sim condition * time + (1|plate)$$

The 0 h time point values were duplicated to account for the absence of a 0 h TGF-β treatment. The model includes:
● An intercept (control condition at 0 h, varying per plate)
● A conditionTGF parameter (TGF-β treatment effect)
● Time parameters for each time point (time12h, time24h, etc.)
● Interaction terms between time and condition (conditionTGF:time12h, conditionTGF:time24h, etc.)

The treatment effect at any given time point is the sum of the relevant parameters (e.g., for TGF-β at 12 h: intercept + conditionTGF + time12h + conditionTGF:time12h).
Average COL1 intensity per cell was calculated for each condition, technical, and biological replicate. Square root transformation was applied to stabilize the variance and improve residual distribution (Piepho 2009). Analysis of variance using type III sum of squares, followed by a post hoc test, was performed to identify significant differences between factor

levels. For visualization, sqrt_mean_int data was normalized per plate by subtracting the 0 h time point values. The resulting data points and model-predicted values were plotted (Figure 1C). The underlying data can be found in Table S8.

5. Acknowledgements

We would like to acknowledge the invaluable contributions of several core facilities and individuals who made this research possible:
[...]
We thank the EMBL Advanced Light Microscopy Facility, notably Aliaksandr Halavatyi, Beate Neumann, and Manuel Gunkel, for their assistance with imaging.

[...]

8. Data and code availability

The mass spectrometry proteomics data have been deposited to the ProteomeXchange Consortium via the PRIDE partner repository with the dataset identifier PXD056096. The transcriptomics sequencing data has been deposited to the ArrayExpress repository with the ArrayExpress accession E-MTAB-14521. Microscopy data are available in the BioStudies [...] All code used to perform the computational analyses described and to reproduce the figures is available at https://github.com/saezlab/kidneyfibrosis_multiomicsmodel_paper All figures and analyses can be reproduced using the provided supplementary tables (contain processed data and analysis results) and the source data provided on Github